Stem Cell Reports
Report
ISSCR
OPEN ACCESS

Single-Cell Mechanical Analysis of Human Pluripotent Stem Cell-Derived Cardiomyocytes for Drug Testing and Pathophysiological Studies

Nimer Ballan,[1] Naim Shaheen,[1] Gordon M. Keller,[2,3] and Lior Gepstein[1,4,*]
[1]Rappaport Faculty of Medicine, Technion-Israel Institute of Technology, POB 9649, Haifa 3109601, Israel
[2]McEwen Stem Cell Institute and Princess Margaret Cancer Center, UHN, Toronto, ON, Canada
[3]Department of Medical Biophysics, University of Toronto, Toronto, ON, Canada
[4]Cardiolology Department, Rambam Health Care Campus, Haifa, Israel
*Correspondence: mdlior@technion.ac.il
https://doi.org/10.1016/j.stemcr.2020.07.006

SUMMARY

Current platforms for studying the mechanical properties of human pluripotent stem cell-derived cardiomyocytes (hPSC-CMs) as single cells do not measure forces directly, require numerous assumptions, and cannot study cell mechanics at different loading conditions. We present a method for directly measuring the active and passive forces generated by single-cell hPSC-CMs at different stretch levels. Utilizing this technique, single hPSC-CMs exhibited positive length-tension relationship and appropriate inotropic, klinotropic, and lusitropic changes in response to pharmacological treatments (isoproterenol and verapamil). The unique potential of the approach for drug testing and disease modeling was exemplified by doxorubicin and omecamtiv mecarbil drug studies revealing their known actions to suppress (doxorubicin) or augment (omecamtiv mecarbil at low dose) cardiomyocyte contractility, respectively. Finally, mechanistic insights were gained regarding the cellular effects of these drugs as doxorubicin treatment led to cellular mechanical alternans and high doses of omecamtiv mecarbil suppressed contractility and worsened the cellular diastolic properties.

INTRODUCTION

The ability to generate human pluripotent stem cell-derived cardiomyocytes (hPSC-CMs) opened new avenues for cardiac disease modeling (Itzhaki et al., 2011; Sun et al., 2012), drug testing (van Meer et al., 2019), and regenerative medicine (Liu et al., 2018; Protze et al., 2017) applications. To achieve these goals, several phenotyping assays were developed, optimized, and utilized to assess the electrophysiological, calcium handling, and mechanical properties of hPSC-CMs at the cellular and tissue levels (Ribeiro et al., 2015; Tiburcy et al., 2017).

To evaluate the cardiomyocyte's contractile properties at the single-cell level and specifically of hPSC-CMs, optical edge detection algorithms were initially used, estimating contractile forces by tracking cardiomyocytes' shortening (Feaster et al., 2015; Kijlstra et al., 2015). More sophisticated methods using micropost arrays (Rodriguez et al., 2014) and traction force microscopy (Ribeiro et al., 2017) track the movement of fiducial markers created by the tension generated on the substrate as a result of cell contraction. Atomic force microscopy was also utilized (Sun et al., 2012), but is limited to measurements from a small cell surface area.

Although providing information regarding hPSC-CMs' mechanics in health and disease, the aforementioned techniques possess inherent limitations: (1) they do not measure forces directly but rather indirectly using numerous assumptions; (2) they are limited with regard to assessment of the diastolic (passive) properties of the cells; and importantly (3) they do not allow to study cell mechanics at preset and different loading conditions.

We developed a method that can overcome these limitations by directly measuring the forces generated from single-cell hPSC-CMs. To this end, we modified a technique first used (Le Guennec et al., 1990) for quantifying forces of primary rodent cardiomyocytes. This technique involves the attachment of an intact rodent cardiomyocyte at its distal ends to carbon fibers (Sugiura et al., 2006). Usually, it combines a stiff fiber (carbon fiber or glass rod) as a length controller, allowing stretching of the cell, and a flexible fiber that bends when the myocyte contracts. Forces are estimated by tracking the deflection of the flexible carbon fiber. Here, we took this strategy a step forward by establishing a new approach that allows to study both the passive and active mechanical properties of single-cell hPSC-CM at different stretch (preload) levels. Following validation of the new approach, we explored its potential role in drug testing and for studying different pathologies.

RESULTS

To measure forces generated by isolated hPSC-CMs two challenges had to be tackled: (1) the relative immature morphology of hPSC-CMs and (2) the inability to attach and manipulate single hPSC-CMs that are adhered to the surface. To address the former challenge, we used an embryoid body (EB) cardiomyocyte differentiation protocol, involving manipulation of the BMP, activin-nodal,

This is an open access article under the CC BY-NC-ND license (http://creativecommons.org/licenses/by-nc-nd/4.0/).

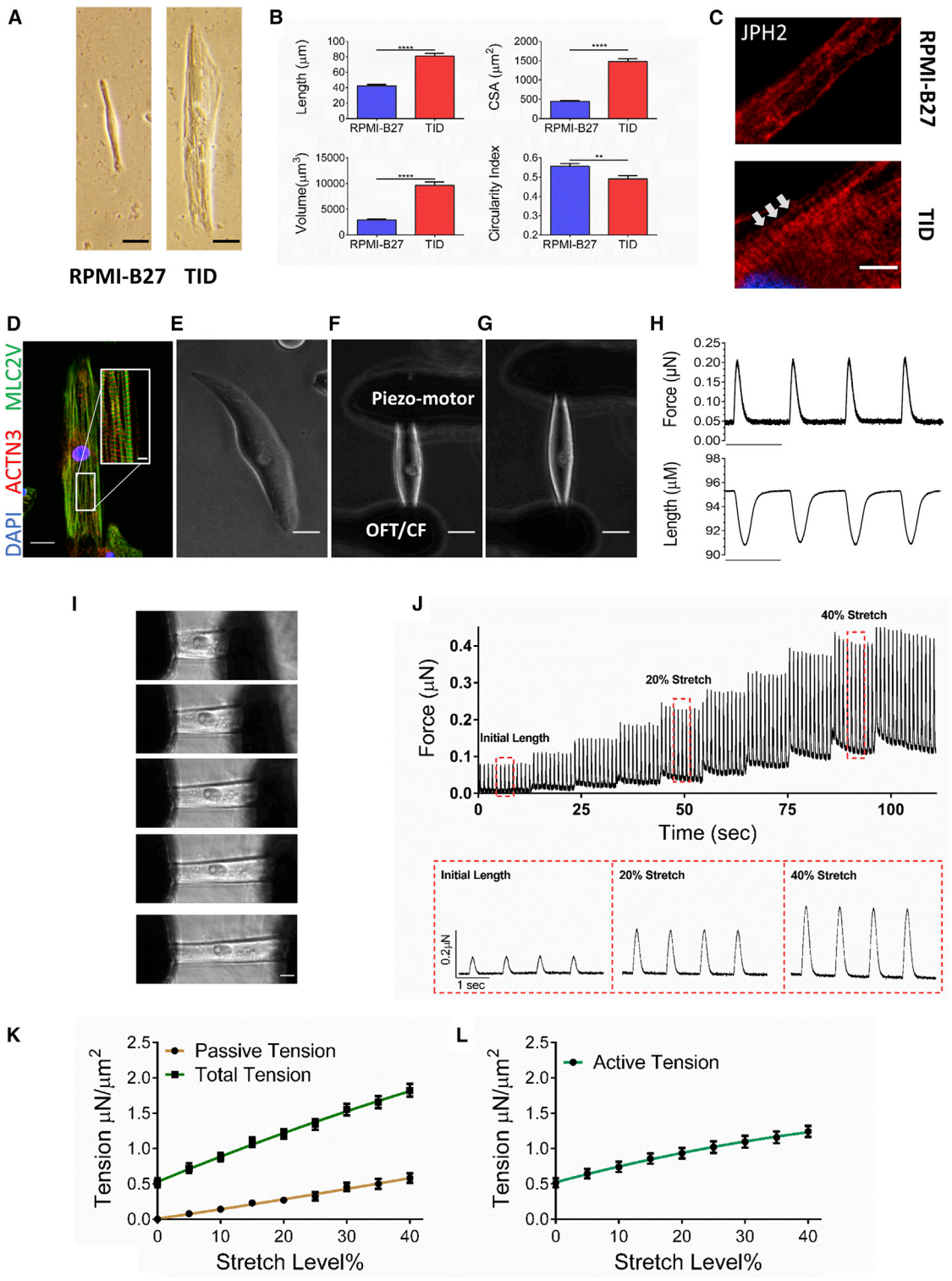

Figure 1. Morphological Maturation and Single-Cell Force Measurements of hPSC-CMs

(A) Bright-field microscopic images of single hPSC-CM after treatment with RPMI-B27 medium (left panel) or with the TID protocol (right). Scale bar, 15 μm.

(legend continued on next page)

and Wnt signaling pathways, to derive ventricular cells from human embryonic stem cells (hESCs) (Figure S1) (Lee et al., 2017).

To achieve further cell maturation, we treated the hPSC-derived ventricular cells with three hormonal factors: triiodo-L-threonine, dexamethasone, and insulin-like growth factor-1 (TID protocol), suggested to promote cardiomyocyte maturation (Birket et al., 2015). This led to robust structural maturation of the hPSC-CMs (Figures 1A–1D), manifested by a significant increase in the cell's major axis length (80.7 ± 3.7 versus 42.4 ± 1.5 μm, $p < 0.0001$), surface area (1,491 ± 67 versus 444 ± 19 μm^2, $p < 0.001$), and volume (9,649 ± 659 versus 2,929 ± 154 μm^3, $p < 0.0001$) (Figure 1C). In addition, the TID-treated cells were characterized by a more elongated shape (lower circularity index: 0.49 ± 0.02 versus 0.55 ± 0.02, $p < 0.01$; Figures 1B and S1C–S1E), by the development of T-tubules (positive staining for junctophilin-2, Figure 1C) and by more organized sarcomeres (advanced striated pattern, Figure 1D).

Measuring forces from single cells was previously done only in primary rodent cardiomyocytes that were already in suspension. In contrast, hPSC-CMs are cultured on a plastic Petri dish or glass coverslip and maintained through integrin-mediated adhesions. To overcome this challenge, dispersed hPSC-CMs were cultured on a collagen-coated substrate for 7 days, where they developed vigorous contractions along their long axis. Cells were then partially detached from the substrate using collagenase and attached, at their distal edges, to two optical/carbon fibers coated with a biological adhesive material. Cells were manipulated to fully detach from the surface using slight lateral movements (Figures 1E and S2A; Video S1). Following this procedure, hPSC-CMs remained intact with preserved morphology (Figures 1E–1G) and contractility for >1 h.

Active and passive forces were measured directly from the attached hPSC-CMs during isometric contraction using a highly sensitive optical force transducer (OFT) (Figures 1H, top panel, 1I and 1J; Video S2), or indirectly by using flexible carbon fibers and tracking their motion during isotonic contraction (Figure 1H, bottom panel). After an initial learning curve (where the carbon fibers were easier to manipulate), we noted that the efficiency (successful attachment >90% of cells) time required (<1 min) for cell attachment, and throughput of the measurements were similar between the two methods. Similarly, measurements using both systems were highly stable over a relatively long period of time (~15 min, Figures S2B and S2C). Finally, while both methods displayed adequate signal-to-noise ratio (SNR) values, the optical edge detection approach was characterized by a higher SNR than the OFT method (Figures S2D and S2E).

To evaluate for length-tension relationships (LTR), hPSC-CMs were sequentially stretched to up to 20%–40% of their initial length using a piezoelectric length controller (Figure 1I) and field stimulated (1 Hz) to induce contraction. The resulting active forces ranged between 30 and 250 nN (Figure 1J). To determine the corresponding tensions, measurements were normalized to the cells' cross-sectional area. All hPSC-CM batches studied exhibited a positive LTR (Frank-Starling law) according to both the OFT and edge detection methods, with both active and passive forces increasing with cell stretching (Figures 1J–1L, S3A–D). The mean active tension measured at baseline cell length was 0.51 ± 0.06 $\mu N/\mu m^2$, with tensions gradually increasing following stretch, reaching 1.24 ± 0.08 $\mu N/\mu m^2$ at 40% stretch (Figure 1L). We also measured the passive (resting) tension of the hPSC-CMs (Figure 1K), which also increased with stretch up to 0.58 ± 0.07 mN/mm^2 (at 40% stretch).

We also evaluated the effect of the TID maturation protocol on the mechanical properties of the treated cells and noted that it resulted in marked enhancement of their contractile properties (Figure S1F). Consequentially, TID

(B) Summary of the changes induced by the TID protocol in the cells' major axis length, surface area, volume, and circularity index (n = 107, 107, 44, and 150, respectively, from 3 or 4 independent experiments) as compared with control RPMI-B27 treatment (n = 103, 103, 32, and 165, respectively, from 3 or 4 independent experiments). ****$p < 0.0001$ (unpaired t test).

(C) Immunostaining of junctophilin-2 (JPH2), a T-tubule marker, in RPMI-B27- and TID-treated cells showing (arrowheads) the striated JPH2 pattern in TID-treated cell. Scale bar, 4 μm.

(D) Co-immunostaining of an hPSC-CM for α-actinin (red), MLC-2V (green), and DAPI (blue). Scale bar, 10 μm.

(E–G) Bright-field microscopy images of plated single-cell hPSC-CM (E); after detachment, lifting and attachment to the coated optical/carbon fibers (F); and following stretching (G).

(H) Representative force measurements using OFT recordings (upper panel) and traces obtained using an edge detection algorithm (bottom).

(I–L) Length-tension relationships of single-cell hPSC-CM. (I) Sequential stretching of single-hPSC-CM using the piezoelectric length controller. Each image shows 10% stretch increments. Scale bar, 8 μm. (J) Continuous force measurements (OFT) at different stretch levels. The red boxes show high-magnifications of the traces obtained at 0%, 20%, and 40% stretch levels. (K and L) Plots describing the relationships between the total (K) (green), passive (K) (orange), and active (L) tensions generated as function of the different stretch levels (n = 11 from 3 independent experiments).

treatment was used in all further studies. Finally, we demonstrated that the length-tension curves observed in the hESC-CMs could also be reproduced in cardiomyocytes derived from a human induced pluripotent stem cell (hiPSC) line (Itzhaki et al., 2011) that were obtained and studied using the same differentiation, TID maturation, and force measurement experimental protocols (Figure S3E).

We next evaluated the ability to detect drug-induced contractility changes by testing the effects of the β-agonist isoproterenol (Figures 2A–2D). The OFT method was used to assess the contractility of hPSC-CMs at three stretch levels (0%, 10%, and 20%). Isoproterenol significantly ($p < 0.001$) increased the force of contraction (FOC) by 38% ± 7%, 27% ± 7%, and 25% ± 8% at these respective stretch levels (Figures 2A and 2B). Isoproterenol also had a positive klinotropic effect, increasing the maximal contraction velocity by 0.43 ± 0.10, 0.58 ± 0.11, and 0.60 ± 0.120 μN/s at 0%, 10%, and 20% stretch levels, respectively ($p < 0.001$, Figure 2C); as well as a positive lusitropic effect, increasing maximal relaxation velocities by 0.35 ± 0.11, 0.40 ± 0.14, and 0.47 ± 0.12 μN/s ($p < 0.001$, Figure 2D).

To evaluate a drug that negatively affects contractility, we tested the calcium channel blocker verapamil (500 nM, Figures 1E–1H). Verapamil significantly ($p < 0.0001$) decreased FOC by 33% ± 7%, 30% ± 6%, and 31% ± 5% relative to baseline values at 0%, 10%, and 20% stretch levels, respectively (Figures 2K–2L). Verapamil also had a negative klinotropic effect, decreasing the respective maximal contraction velocities by 0.24 ± 0.11, 0.26 ± 0.12, and 0.30 ± 0.11 μN/s ($p < 0.001$, Figure 2M); as well as a negative lusitropic effect, decreasing maximal relaxation velocities by 0.16 ± 0.06, 0.20 ± 0.06, and 0.25 ± 0.06 μN/s ($p < 0.001$, Figure 2N).

To evaluate the role of the new approach in studying clinically relevant pathologies, we exposed the hPSC-CMs to the cardiotoxic chemotherapeutic agent, doxorubicin (Dox) (3μM). Dox-treated hPSC-CMs displayed disrupted sarcomeres with reduced myofibrillar content when stained for α-actinin and MLC-2V (Figure 3A). Importantly, the cells also exhibited reduced active tensions and impaired klinotropic properties, compared with vehicle-treated cells. This was evident at all stretch levels ($p < 0.01$, Figures 3B and 3C) with the Dox-treated cells also showing a more flattened LTR curve (Figures 3B and 3C).

Interestingly, 42% of Dox-treated hESC-CMs (in contrast to 8% of vehicle-treated cells, $p < 0.05$) displayed mechanical alternans (Figures 3D and 3E; Video S3), which became even more abnormal at higher pacing frequencies (Figure 3D). Similar results were also obtained in hiPSC-CMs, in which mechanical alternans was observed in 62% of the cells analyzed ($n = 16$, Figure S4A), in contrast to 7% in the vehicle control group ($n = 12$, $p < 0.05$). To further investigate the mechanisms underlying mechanical alternans, we expressed the fluorescent calcium indicator, GCAMP6f (Shinnawi et al., 2015) in the cells to evaluate their calcium-handling properties. Dox-treated hESC-CMs showed significant intracellular calcium transient abnormalities (Figures S4B and S4C), a phenomenon that may be responsible for the observed mechanical alternans.

We next evaluated the impact of omecamtiv mecarbil (OM), a positive inotropic agent currently in phase 3 clinical trial for heart failure treatment (Cleland et al., 2011). OM affects acto-myosin interactions by increasing the propensity of the strong bound state and therefore can augment contractility (Woody et al., 2018). We evaluated the mechanical properties of single-cell hPSC-CMs using the optical edge detection method (Figure 4A) at baseline and after OM treatment. Application of 0.1 μM OM significantly increased active force by ~11% ($p < 0.001$) with minimal effects on contraction and relaxation velocities (Figures 4C and 4D). Surprisingly, application of higher OM doses (1 and 10 μM), which may still be relevant clinically, significantly suppressed contractility. Consequentially, 1 μM OM decreased both cell shortening (by ~30%, $p < 0.05$) and maximal contraction and relaxation velocities (Figures 4A and 4B). In contrast, OM displayed a dose-response effect in prolonging contraction and relaxation times (Figures 4E and 4F), a finding consistent with its known effects.

We also assessed the passive tensions generated in the OM-treated (10 μM) hPSC-CMs using the protocol defined in Figures S4D and S4E, and noted significant increases in resting tension values (Figure 4G). This diastolic abnormality became even more prominent at higher stretch levels. To elucidate the mechanisms underlying the latter finding, treated and non-treated cells were immunostained for α-actinin, enabling assessment of sarcomere length. We found that high OM doses (10 μM) decreases sarcomere length (Figures S4F and S4G, $p < 0.0001$) in accordance with the hypothesis that OM increases intracellular tension (Ribeiro et al., 2017).

DISCUSSION

The advent of hPSC technologies provided exciting new tools for cardiac research. One of the shortcomings in this field, however, is the lack of methodology to study the active and passive mechanical properties of hPSC-CMs at the single-cell level. To address this important unmet need, we combined hPSC differentiation and maturation protocols to derive morphological mature ventricular cells, with a unique single-cell mechanical analysis methodology. Using this approach, we were able to directly measure the active and passive tensions of single-cell hPSC-CMs at different loading conditions.

Both techniques used in the current study to evaluate the mechanical properties of hPSC-CMs (the carbon fiber

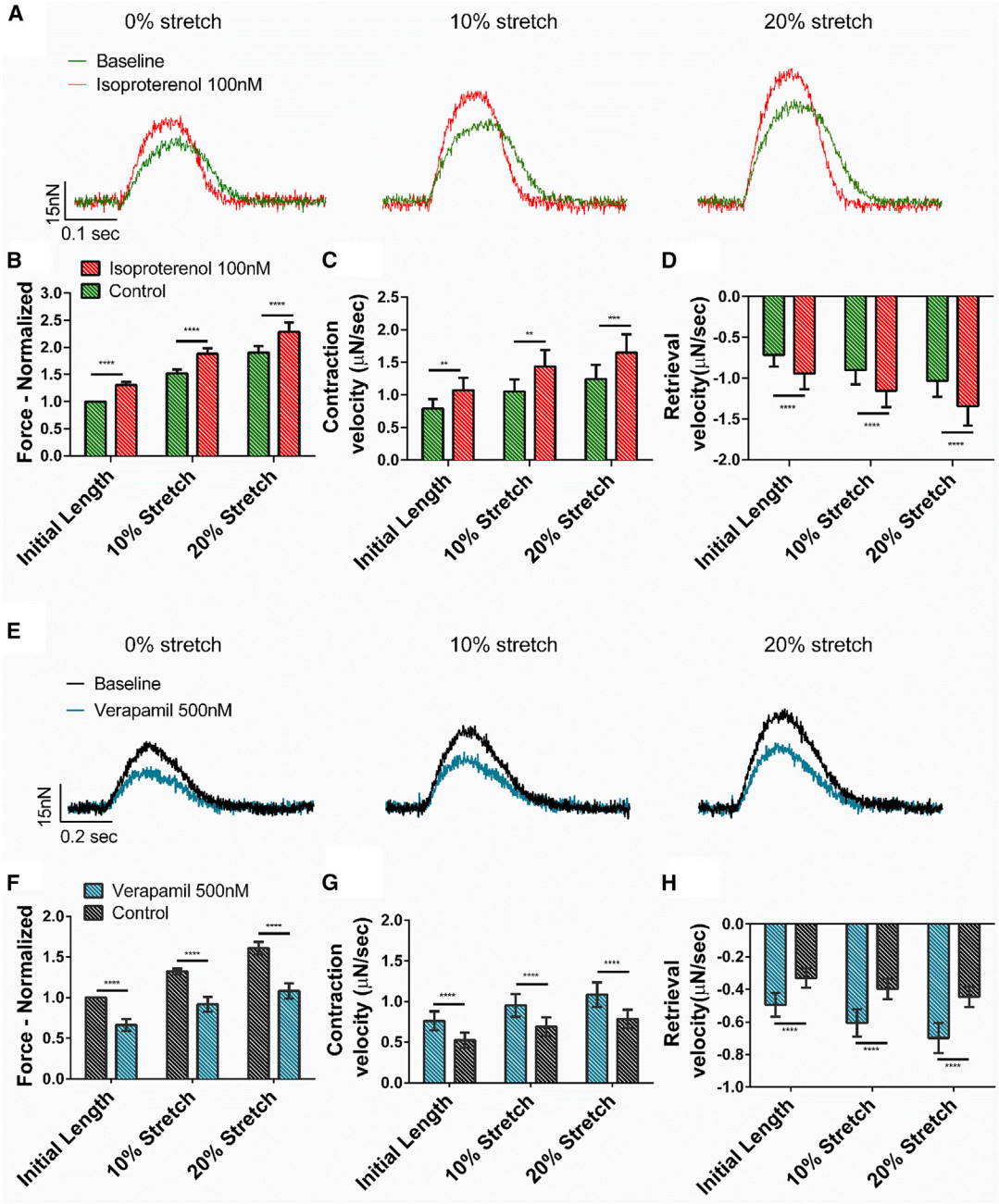

Figure 2. Pharmacological Effects on the Single-Cell Contractile Properties of hPSC-CMs

(A) Representative force traces, measured at 0%, 10%, and 20% stretch level, before (green) and after (red) isoproterenol (100 nM) treatment.

(B–D) Summary of isoproterenol effects on force amplitude (relative change) (B), maximal contraction velocity (C), and maximal relaxation velocity (D) at the different stretch levels (n = 21 cells from 4 independent experiments).

(E) Representative force traces before (black) and after (blue) verapamil (500 nM) treatment.

(F–H) Summary of verapamil effects on force amplitude (relative changes) (F) and maximal contraction (G) and relaxation (H) velocities (n = 17 from 4 independent experiments). Note the typical positive and negative inotropic, klinotropic, and lusinotropic responses induced by isoproterenol and verapamil, respectively.

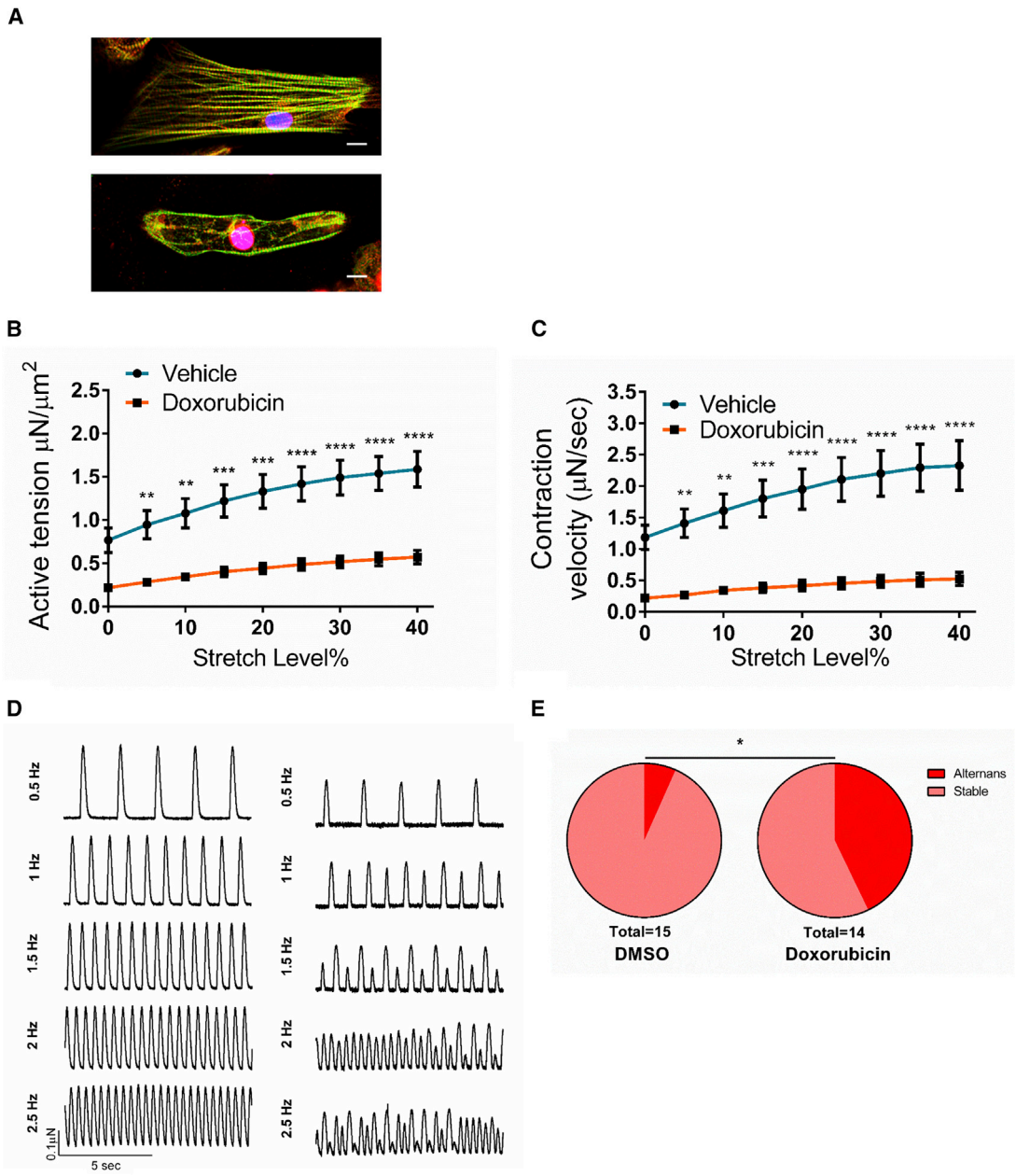

Figure 3. Doxorubicin Effects on the Mechanical Properties of hPSC-CMs

(A) Representative immunofluorescence staining of the vehicle- (top panel) and Dox-treated (bottom) hPSC-CMs for sarcomeric α-actinin (red), MLC-2V (green), and DAPI (blue). Scale bar, 10 μm. Note the resulting sarcomeric destruction and disarray.

(B and C) Plots presenting the length-tension relationship (B) and the maximal contraction velocities (C) of vehicle-treated hPSC-CMs (blue, n = 15 from 4 independent experiments) and Dox-treated hPSC-CMs (orange, n = 14 from 4 experiments). Differences between Dox and vehicle groups were analyzed by two-way ANOVA and the Holm-Sidak multiple comparison test. *$p < 0.05$, **$p < 0.01$.

(D) Representative force measurements from vehicle control and Dox-treated groups. Notice the mechanical alternans in the Dox-treated hPSC-CMs, especially at faster pacing rates.

(E) Percentage of cells with mechanical alternans, which was significantly higher ($p < 0.05$, chi-square test) in the Dox-treated cells (n = 11 and n = 8 for the vehicle- and Dox-treated cells, respectively, from three independent experiments).

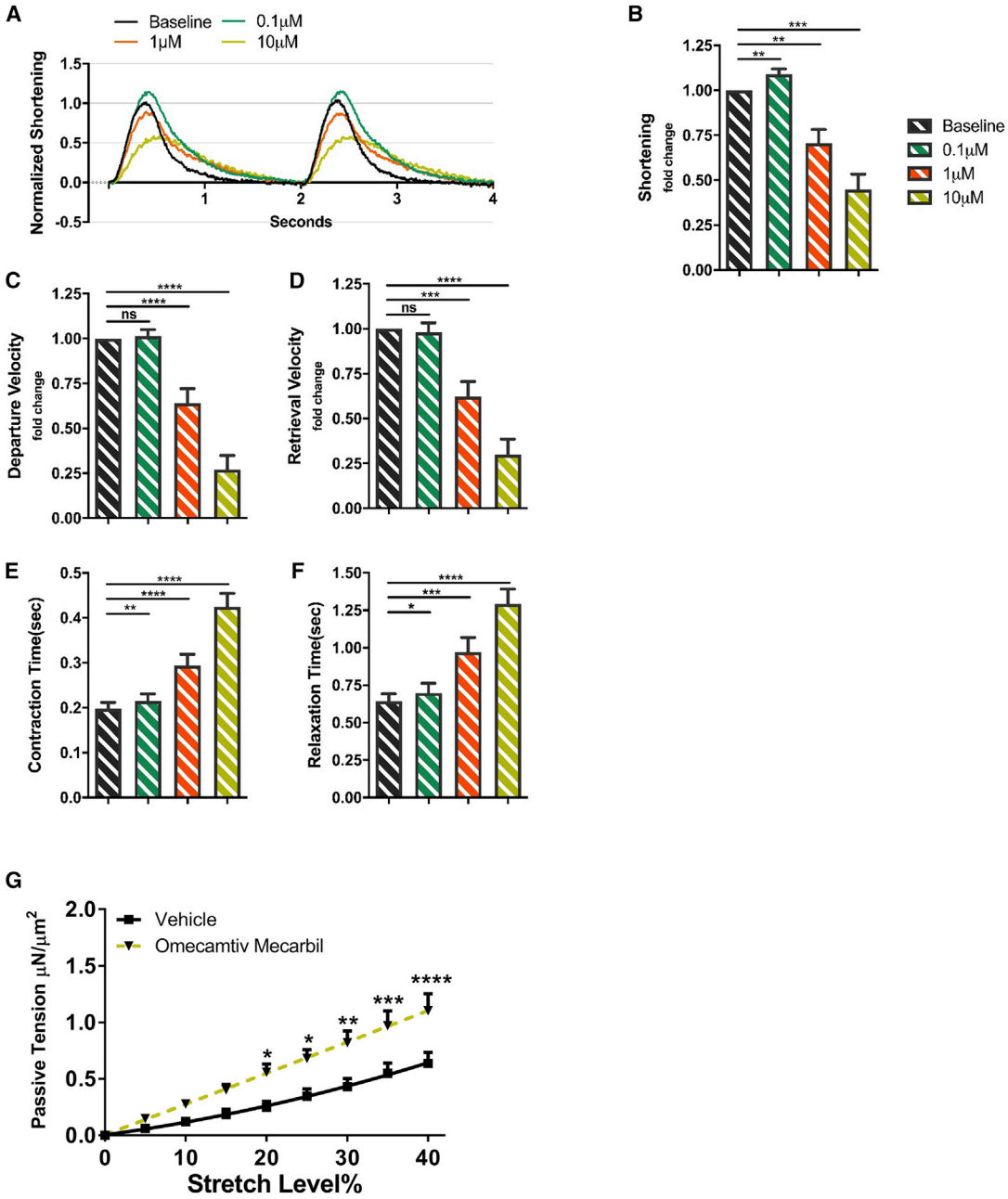

Figure 4. Omecamtiv Mecarbil Effects on the Active and Passive Mechanical Properties of Single-Cell hPSC-CMs

(A) Typical normalized mechanical tracings obtained from the omecamtiv mecarbil (OM)-treated hPSC-CMs using the optical edge detection module.

(B–F) Plots summarizing changes in the following mechanical parameters: normalized shortening amplitude (B), contraction velocity (C), relaxation velocity (D), contraction time (E), and relaxation time (F) following application of 0.1, 1, 10 μM of OM. n = 20 cells in each group from 5 independent experiments.

(G) Evaluation of the passive tensions measured in OM-treated (1 μM; green; n = 10 from 4 independent experiments) hPSC-CMs as compared with the vehicle control group (black, n = 13 from 4 experiments). Differences between the groups for each OM concentration were analyzed by one-way ANOVA and the Holm-Sidak multiple comparison test. **p < 0.01, ***p < 0.001, ****p < 0.0001.

edge detection and the OFT) were found to be highly reliable and reproducible, enabling continuous and stable measurements with high SNR, detecting changes as small as 10 nN. In addition to detecting changes in the FOC (ionotropic changes) of hPSC-CMs, the new approach also allowed to evaluate alterations in the rate of contraction and relaxation (klinotropic and lusitropic effects, respectively). Most importantly, however, is the ability to manipulate cell length, allowing to characterize the mechanical properties of the cells at different stretch (preload) levels. Our results reveal a positive LTR (consistent with the Frank-Starling law) in both hESC-CMs and hiPSC-CMs, manifested by an increase in both the active and passive tensions following stretch, a phenomenon that was not validated before in single-cell hPSC-CMs.

To derive cells with the appropriate morphological properties for force measurements (elongated, "brick-shaped," ventricular cells with anisotropic sarcomeric alignment) we used a previously described hormonal-based maturation protocol, combining thyroid hormone (T3), IGF-1, and dexamethasone (Birket et al., 2015). This protocol was shown to enhance maturation of hPSC-CMs at the electrophysiological, electrical-contraction coupling, bioenergetics, and ultrastructural levels (Birket et al., 2015; Parikh et al., 2017). In the current study a similar protocol led, in addition to the observed ultrastructural maturation (reduced circularity index coupled with an increase in the cells' dimensions, sarcomeric organization, and T-tubule formation), to augmentation of the cellular contractile properties as manifested by a left upward shift in the LTR curve in the TID-treated hPSC-CMs.

Several forms of inherited and acquired cardiac disease can alter the passive mechanical properties of the myocardium, leading to heart failure with preserved ejection fraction. The passive myocardial stiffness is determined by two components: the extracellular matrix (ECM) and the cardiomyocytes. Thus, diastolic abnormalities may stem from either abnormal ECM depositions or fibrosis (Franssen and Gonzalez Miqueo, 2016) or from alterations in the inherent cardiomyocytes' properties. The latter can result from altered expression of Titin isoforms or changes in Titin's phosphorylation and oxidative states (Franssen and Gonzalez Miqueo, 2016); changes in acto-myosin interactions and regulation (King et al., 2011); or alterations in post-translational modification of microtubules (Chen et al., 2018).

Experimental approaches evaluating the passive mechanical properties primarily focus at the tissue level: studying the intact heart, *ex-vivo*-explanted tissue models, or engineered tissues derived from hPSC-CMs. This prevents assessment of the relative contributions of ECM changes versus alterations in the cardiomyocyte's mechanical properties. By measuring passive tensions in hPSC ventricular cells at different stretch levels, we can now isolate the relative contribution of alterations in the cardiomyocyte's passive mechanical properties. Using this approach, we identified increased cellular stiffness in hPSC-CMs as a result of alterations of acto-myosin interactions induced by high-concentration OM treatment. Interestingly, hints for similar OM effects on the cardiac passive mechanical properties were already found in a rat model (Nagy et al., 2015).

We next highlighted the unique potential of this new approach for drug studies and for modeling of clinically relevant pathologies by exposing the cells to the anti-cancer agent Dox, to adrenergic stimulation (isoproterenol), to a calcium channel blocker (verapamil), and to escalating doses of the positive inotropic agent OM. Our results recapitulated the known clinical effects of these interventions in suppressing (Dox, verapamil) or augmenting (OM at low dose and isoproterenol) cardiomyocyte contractility. Importantly, novel insights were gained, as Dox treatment also led to cellular mechanical alternans and high doses of OM, rather than improving the mechanical properties of the cells, suppressed the amplitude and kinetics of the active forces produced by the cells and worsened the cellular diastolic properties. The latter finding, warrants further investigations, as OM is current being evaluated in advanced clinical studies.

The cellular mechanical alternans identified in our study in both hESC-CMs and hiPSC-CMs after Dox treatment was accompanied by (and probably stems from) abnormal calcium-handling dynamics. These calcium abnormalities can be attributed to redox modification of the SR (Terentyev et al., 2008) or to APD modulation (Fernandez-Chas et al., 2018) as a result of Dox treatment. Importantly, the irregular calcium transients identified may also lead to the increased arrhythmogenicity and enhanced cytotoxicity, associated clinically with Dox cardiotoxicity.

The new approach for direct force measurements of hPSC-CMs could be coupled, in the future, with additional assays, such as single-cell imaging of excitation-contraction coupling and single-cell gene expression analysis to provide further mechanistic insights into various physiological/pathophysiological phenomena. Moreover, this approach can be implemented to investigate mechanistic effects of drugs and pathological conditions that cannot be unveiled in tissue preparations (Robison et al., 2016) and unloaded cardiomyocytes (Yasuda et al., 2005). Consequentially, the described method and the results of the current study may have important implications for the fields of cardiac physiology, mechano- and cellular biology, and to the emerging fields of cardio-oncology and heart failure treatments.

EXPERIMENTAL PROCEDURES

Supplemental expanded Experimental Procedures section is available online.

hESC Propagation, Cardiomyocyte Differentiation, and Maturation

Studies were performed using the HES3-NKX2-5$^{GFP/W}$ hESC line (gift from Prof. Elefanty) and a previously established hiPSC line (Itzhaki et al., 2011), derived according to the approval of the IRB (Helsinki) committee of Rambam Medical Center.. The growth factor, EB-based differentiation process to derive ventricular cardiomyocytes was described elsewhere (Lee et al., 2017). At day 22, beating EBs were dissociated into single cells and seeded on collagen-coated substrate at a density of 15,000–18,000 cells/cm^2. To promote maturation, cells were cultured with TID medium containing: RPMI medium supplemented with 2% B27 with insulin (Gibco), 3,3′,5-triiodo-L-thyronine sodium salt, LONG R3 IGF-I human, dexamethasone and 1% penicillin/streptomycin.

Single-Cell Force Measurements

The single-cell force measurement system was built on an Olympus IX51 epifluorescence microscope and consists of two micro-manipulators (MyoStretcher System, IonOptix) connected to an OFT (OptiForce, IonOptix) and a piezoelectric length controller. The 10 μm diameter carbon/optical fibers were coated with a biological adhesive material (MyoTak, IonOptix). Cells were stretched to different initial lengths and field stimulated at 1 Hz. If not mentioned otherwise, all force measurement studies were conducted on TID-treated cells.

Cell Attachment Procedure

To be selected for force measurement, the single hPSC-CM had to display elongated shape and anisotropic contraction along its long axis. Following enzymatic (type 2 collagenase) dissociation, the hPSC-CM attachment procedure to the fibers consisted of three major steps: (1) attaching the coated fibers to the cell at its two distal edges; (2) separating the cell to fully detach from the substrate through the use of slight lateral movements by pulling the attached cell to one side; and (3) lifting the fully attached hPSC-CM for further inspection (Figure S2A; Video S1).

Pharmacological Studies

The effects of isoproterenol (100 nM) and verapamil (500 nM) were evaluated by measuring the contraction forces generated by a single hPSC-CM before and after drug treatment. For Dox studies, hPSC-CM were treated with Dox-containing medium (3 μM) for 24 h. The vehicle group was treated with 0.3% DMSO medium. For OM experiments, baseline recordings were followed by incubation of the cells with escalating drug concentrations (0.1, 1, and 10 μM).

SUPPLEMENTAL INFORMATION

Supplemental Information can be found online at https://doi.org/10.1016/j.stemcr.2020.07.006.

AUTHOR CONTRIBUTION

N.B. was responsible for research design, method development, execution, performing the experiments, data analysis, and manuscript preparation. N.S. contributed to data research design and method development. G.M.K. was responsible for the hPSC ventricular cells derivation. L.G. was responsible for conceptual and research design, supervision, and manuscript preparation.

DECLARATION OF INTERESTS

G.M.K. is a scientific founder and paid consultant for BlueRock Therapeutics LP, a paid consultant for VistaGen Therapeutics and a board member of Anagenesis Biotechnologies..

ACKNOWLEDGMENTS

This work was supported by the European Research Council (ERC-2017-COG-773181-iPS-ChOp-AF), by the Israel Scientific Foundation (ISF-1088/18), and by the Technion-UHN research fund

Received: October 26, 2019
Revised: July 8, 2020
Accepted: July 8, 2020
Published: August 6, 2020

REFERENCES

Birket, M.J., Ribeiro, M.C., Kosmidis, G., Ward, D., Leitoguinho, A.R., van de Pol, V., Dambrot, C., Devalla, H.D., and Davis, R.P. (2015). Contractile defect caused by mutation in MYBPC3 revealed under conditions optimized for human PSC-cardiomyocyte function. Cell Rep. *13*, 733–745.

Chen, C.Y., Caporizzo, M.A., Bedi, K., Vite, A., Bogush, A.I., Robison, P., Heffler, J.G., Salomon, A.K., Kelly, N.A., Babu, A., and Morley, M.P. (2018). Suppression of detyrosinated microtubules improves cardiomyocyte function in human heart failure. Nat. Med. *24*, 1225–1233.

Cleland, J.G., Teerlink, J.R., Senior, R., Nifontov, E.M., Mc Murray, J.J., Lang, C.C., Tsyrlin, V.A., Greenberg, B.H., Mayet, J., Francis, D.P., et al. (2011). The effects of the cardiac myosin activator, omecamtiv mecarbil, on cardiac function in systolic heart failure: a double-blind, placebo-controlled, crossover, dose-ranging phase 2 trial. Lancet *378*, 676–683.

Feaster, T.K., Cadar, A.G., Wang, L., Williams, C.H., Chun, Y.W., Hempel, J.E., Bloodworth, N., Merryman, W.D., Lim, C.C., Wu, J.C., et al. (2015). Matrigel mattress: a method for the generation of single contracting human-induced pluripotent stem cell-derived cardiomyocytes. Circ. Res. *117*, 995–1000.

Fernandez-Chas, M., Curtis, M.J., and Niederer, S.A. (2018). Mechanism of doxorubicin cardiotoxicity evaluated by integrating multiple molecular effects into a biophysical model. Br. J. Pharmacol. *175*, 763–781.

Franssen, C., and Gonzalez Miqueo, A. (2016). The role of titin and extracellular matrix remodelling in heart failure with preserved ejection fraction. Neth. Heart J. *24*, 259–267.

Itzhaki, I., Maizels, L., Huber, I., Zwi-Dantsis, L., Caspi, O., Winterstern, A., Feldman, O., Gepstein, A., Arbel, G., Hammerman, H.,

et al. (2011). Modelling the long QT syndrome with induced pluripotent stem cells. Nature *471*, 225–229.

Kijlstra, J.D., Hu, D., Mittal, N., Kausel, E., van der Meer, P., Garakani, A., and Domian, I.J. (2015). Integrated analysis of contractile kinetics, force generation, and electrical activity in single human stem cell-derived cardiomyocytes. Stem Cell Reports *5*, 1226–1238.

King, N.M., Methawasin, M., Nedrud, J., Harrell, N., Chung, C.S., Helmes, M., and Granzier, H. (2011). Mouse intact cardiac myocyte mechanics: cross-bridge and titin-based stress in unactivated cells. J. Gen. Physiol. *137*, 81–91.

Le Guennec, J.Y., Peineau, N., Argibay, J.A., Mongo, K.G., and Garnier, D. (1990). A new method of attachment of isolated mammalian ventricular myocytes for tension recording: length dependence of passive and active tension. J. Mol. Cell Cardiol. *22*, 1083–1093.

Lee, J.H., Protze, S.I., Laksman, Z., Backx, P.H., and Keller, G.M. (2017). Human pluripotent stem cell-derived atrial and ventricular cardiomyocytes develop from distinct mesoderm populations. Cell Stem Cell *21*, 179–194 e174.

Liu, Y.W., Chen, B., Yang, X., Fugate, J.A., Kalucki, F.A., Futakuchi-Tsuchida, A., Couture, L., Vogel, K.W., Astley, C.A., Baldessari, A., et al. (2018). Human embryonic stem cell-derived cardiomyocytes restore function in infarcted hearts of non-human primates. Nat. Biotechnol. *36*, 597–605.

Nagy, L., Kovacs, A., Bodi, B., Pasztor, E.T., Fulop, G.A., Toth, A., Edes, I., and Papp, Z. (2015). The novel cardiac myosin activator omecamtiv mecarbil increases the calcium sensitivity of force production in isolated cardiomyocytes and skeletal muscle fibres of the rat. Br. J. Pharmacol. *172*, 4506–4518.

Parikh, S.S., Blackwell, D.J., Gomez-Hurtado, N., Frisk, M., Wang, L., Kim, K., Dahl, C.P., Fiane, A., Tønnessen, T., Kryshtal, D.O., et al. (2017). Thyroid and glucocorticoid hormones promote functional t-tubule development in human-induced pluripotent stem cell-derived cardiomyocytes. Circ. Res. *121*, 1323–1330.

Protze, S.I., Liu, J., Nussinovitch, U., Ohana, L., Backx, P.H., Gepstein, L., and Keller, G.M. (2017). Sinoatrial node cardiomyocytes derived from human pluripotent cells function as a biological pacemaker. Nat. Biotechnol. *35*, 56–68.

Ribeiro, A.J., Ang, Y.S., Fu, J.D., Rivas, R.N., Mohamed, T.M., Higgs, G.C., Srivastava, D., and Pruitt, B.L. (2015). Contractility of single cardiomyocytes differentiated from pluripotent stem cells depends on physiological shape and substrate stiffness. Proc. Natl. Acad. Sci. U S A *112*, 12705–12710.

Ribeiro, A.J.S., Schwab, O., Mandegar, M.A., Ang, Y.S., Conklin, B.R., Srivastava, D., and Pruitt, B.L. (2017). Multi-imaging method to assay the contractile mechanical output of micropatterned human iPSC-derived cardiac myocytes. Circ. Res. *120*, 1572–1583.

Robison, P., Caporizzo, M.A., Ahmadzadeh, H., Bogush, A.I., Chen, C.Y., Margulies, K.B., Shenoy, V.B., and Prosser, B.L. (2016). Detyrosinated microtubules buckle and bear load in contracting cardiomyocytes. Science *352*, aaf0659.

Rodriguez, M.L., Graham, B.T., Pabon, L.M., Han, S.J., Murry, C.E., and Sniadecki, N.J. (2014). Measuring the contractile forces of human induced pluripotent stem cell-derived cardiomyocytes with arrays of microposts. J. Biomech. Eng. *136*, 051005.

Shinnawi, R., Huber, I., Maizels, L., Shaheen, N., Gepstein, A., Arbel, G., Tijsen, A.J., and Gepstein, L. (2015). Monitoring human-induced pluripotent stem cell-derived cardiomyocytes with genetically encoded calcium and voltage fluorescent reporters. Stem Cell Reports *5*, 582–596.

Sugiura, S., Nishimura, S., Yasuda, S., Hosoya, Y., and Katoh, K. (2006). Carbon fiber technique for the investigation of single-cell mechanics in intact cardiac myocytes. Nat. Prot. *1*, 1453–1457.

Sun, N., Yazawa, M., Liu, J., Han, L., Sanchez-Freire, V., Abilez, O.J., Navarrete, E.G., Hu, S., Wang, L., Lee, A., and Pavlovic, A. (2012). Patient-specific induced pluripotent stem cells as a model for familial dilated cardiomyopathy. Sci. Transl Med. *4*, 130ra147.

Terentyev, D., Gyorke, I., Belevych, A.E., Terentyeva, R., Sridhar, A., Nishijima, Y., Carcache de Blanco, E., Khanna, S., Sen, C.K., Cardounel, A.J., and Carnes, C.A. (2008). Redox modification of ryanodine receptors contributes to sarcoplasmic reticulum Ca^{2+} leak in chronic heart failure. Cir Res. *103*, 1466–1472.

Tiburcy, M., Hudson, J.E., Balfanz, P., Schlick, S., Meyer, T., Liao, M.L., Levent, E., Raad, F., Zeidler, S., Wingender, E., and Riegler, J. (2017). Defined engineered human myocardium with advanced maturation for applications in heart failure modeling and repair. Circulation *135*, 1832–1847.

van Meer, B.J., Krotenberg, A., Sala, L., Davis, R.P., Eschenhagen, T., Denning, C., Tertoolen, L.G., and Mummery, C.L. (2019). Simultaneous measurement of excitation-contraction coupling parameters identifies mechanisms underlying contractile responses of hiPSC-derived cardiomyocytes. Nat. Commun. *10*, 4325.

Woody, M.S., Greenberg, M.J., Barua, B., Winkelmann, D.A., Goldman, Y.E., and Ostap, E.M. (2018). Positive cardiac inotrope omecamtiv mecarbil activates muscle despite suppressing the myosin working stroke. Nat. Commun. *9*, 3838.

Yasuda, S., Townsend, D., Michele, D.E., Favre, E.G., Day, S.M., and Metzger, J.M. (2005). Dystrophic heart failure blocked by membrane sealant poloxamer. Nature *436*, 1025–1029.